Inorganic Chemistry

Article

pubs.acs.org/IC

# Tuning MOF Stability and Porosity via Adding Rigid Pillars

Yan-Xi Tan,[†] Yan-Ping He,[†] and Jian Zhang*[,†]

[†]State Key Laboratory of Structural Chemistry, Fujian Institute of Research on the Structure of Matter, The Chinese Academy of Sciences, Fuzhou, Fujian 350002, P. R. China

Supporting Information

**ABSTRACT:** High stability and permanent porosity are the premise of general applicability for metal−organic framework materials (MOFs). By varying degrees of success on increasing the connectivity of the linear pillar 4,4′-bipyridine (bpy), two isostructural flexible frameworks $[M_2(obb)_2(DMF)_2]\cdot 2DMF$ (**1**, M = Zn or Cu; $H_2obb$ = 4,4′-oxybis(benzoic acid), DMF = N,N-dimethylformamide) with no gas sorption are structurally modified into two rigid frameworks $[Zn_2(obb)_2(bpy)]\cdot DMF$ (**2**) and $[Cu_2(obb)_2(bpy)_{0.5}(DMF)]\cdot 2DMF$ (**3**) with notable gas sorption and separation properties. Especially for **3**, it exhibits gas selective uptake for the adsorption of $CO_2$ over $N_2$ and $CH_4$ under 273 K and has an interesting physically lock effect in benzene and cyclohexane sorption. The results provide a successful strategy on tuning framework stability of flexible structures via adding rigid pillars.

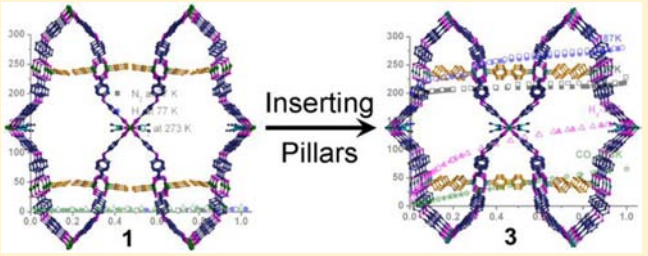


## INTRODUCTION

Porous coordination polymers (PCPs) or metal−organic frameworks (MOFs) with well-defined channels or pores have been receiving intensive research interest because of their aesthetic framework structures and potential applications in gas storage/separation and catalysis.[1,2] For a general applicability, MOFs should have high thermal stability to keep permanent porosity after removal of solvent molecules.[3,4] However, it is a big weakness for most MOFs with large pores which are much easier to collapse or shrink into nonporous frameworks after guest removal.[4a] Therefore, how to retain the pores and avoid the structural shrinking may be extremely challenging. Interpenetration and coordinatively linking interpenetrated frameworks have been demonstrated as the effective chemical approaches for this aim.[5] Moreover, several activated treatment methods, such as solvent-exchange, supercritical $CO_2$, and freeze-drying treatment, have been recognized as other effective physical approaches.[6]

In this contribution, we provide a new idea for tuning MOF stability and porosity via inserting pillars. It is very easy to image that a big room without any pillars would not be stable, and additional pillars should dramatically improve its stability. Although such a simple idea may be known by everybody, to our knowledge, which is rarely used for MOFs to tune their stability and porosity.

Here, such an idea is utilized to optimize MOF stability and its adsorption properties. In this work, we report the synthesis, structural characterizations, and sorption properties of four new MOFs based on a V-shaped 4,4′-oxybis(benzoic acid) (= $H_2obb$) ligand, namely $[M_2(obb)_2(DMF)_2]\cdot 2DMF$ (**1**, M = Zn or Cu); DMF = N,N-dimethylformamide), $[Zn_2(obb)_2(bpy)]\cdot DMF$ (**2**; bpy =4,4′-bipyridine), and $[Cu_2(obb)_2(bpy)_{0.5}(DMF)]\cdot 2DMF$ (**3**). All four compounds consist of paddle-wheel $M_2(COO)_4$ building units linked by the obb ligands, but they exhibit distinct structural topologies because of the attendance of auxiliary bpy ligands. One prominent feature of this work is the structural relationship between an unstable flexible framework of **1** and a much rigid framework of **3**. Although there are large potential free spaces in the framework of **1**, it tends to shrink after the removal of solvent molecules and shows nonpore for gases. Once the bpy pillars are inserted into this similar framework, the resulting framework **3** is very rigid and good for gas storage and separation. The framework of **3** exhibits gas selective uptake of $CO_2$ over $CH_4$. Moreover, an interesting physically lock effect is observed in benzene and cyclohexane sorption for **3**. The results provide a successful strategy on tuning framework stability of flexible structures via inserting rigid pillars.

## EXPERIMENTAL SECTION

**General Procedures.** All reagents were purchased commercially and used without further purification. All Powder X-ray diffraction (PXRD) analyses were recorded on a Rigaku Dmax2500 diffractometer with Cu K$\alpha$ radiation ($\lambda$ = 1.54056 Å) with a step size of 0.05°. Thermal stability studies were carried out on a NETSCHZ STA-449C thermoanalyzer with a heating rate of 10 °C/min under a nitrogen atmosphere. Gas adsorption measurement was performed in the ASAP (Accelerated Surface Area and Porosimetry) 2020 System, and the weight of samples were 0.1079 g for **1-Zn-ht**, 0.1288 g for **1-Cu-ht**, 0.1963 g for **2-ht**, and 0.2156 g for **3-ht**. To obtain reliable $N_2$ uptake at 273 K, the other weight of 0.5531 g for **3-ht** was prepared for measurement.

**Synthesis of $[Zn_2(obb)_2(DMF)_2]\cdot 2DMF$ (1-Zn).** $H_2obb$ (256 mg, 1 mmol) and $Zn(NO_3)_2\cdot 6H_2O$ (297 mg, 1 mmol) were dissolved in

Received: April 16, 2012
Published: August 24, 2012

   dx.doi.org/10.1021/ic300778m | Inorg. Chem. 2012, 51, 9649−9654

DMF/EtOH (2:1, v/v), which were placed in a small vial. The mixture was heated at 80 °C for 5 days, cooled to room temperature, and then placed in the vial for seven days. Colorless block crystals of the product were formed and collected by filtration and washed with DMF several times (Yield: 55 mg, 15%, based on $H_2$obb). Elemental analysis calcd (%) for **1-Zn**: C 50.98, H 4.91, N 6.02; found C 51.35, H 4.74, N 5.99.

**Synthesis of $[Cu_2(obb)_2(DMF)_2]\cdot 2DMF$ (1-Cu).** $H_2$obb (256 mg, 1 mmol) and $Cu(NO_3)_2\cdot 6H_2O$ (297 mg, 1 mmol) were dissolved in DMF, which were placed in a small vial. The mixture was heated at 120 °C for 2 days and then cooled to room temperature. Blue block crystals of the product were formed and collected by filtration and washed with DMF several times (Yield: 230 mg, 63%, based on $H_2$obb). Elemental analysis calcd (%) for **1-Cu**: C 51.73, H 4.58, N 6.25; found C 51.55, H 4.76, N 6.01.

**Synthesis of $[Zn_2(obb)_2(bpy)]\cdot DMF$ (2).** $H_2$obb (256 mg, 1 mmol), 4,4′-bipyridine (78 mg, 0.5 mmol), and $Zn(NO_3)_2\cdot 6H_2O$ (297 mg, 1 mmol) were dissolved in DMF/EtOH (2:1, v/v), which were placed in a small vial. The mixture was heated at 100 °C for 3 days and then cooled to room temperature. Colorless block crystals of the product were formed and collected by filtration and washed with DMF several times (Yield: 350 mg, 81%, based on $H_2$obb). Elemental analysis calcd (%) for **2**: C 56.25, H 4.08, N 12.59; found C 56.44, H 4.18, N 12.46.

**Synthesis of $[Cu_2(obb)_2(bpy)_{0.5}(DMF)]\cdot 2DMF$ (3).** $H_2$obb (256 mg, 1 mmol), 4,4′-bipyridine (78 mg, 0.5 mmol), and $Cu(NO_3)_2\cdot 6H_2O$ (240 mg, 1 mmol) were dissolved in 4 mL of DMF, which were placed in a small vial. The mixture was heated at 120 °C for 2 days and then cooled to room temperature. Blue needle crystals of the product were formed and collected by filtration and washed with DMF several times (Yield: 280 mg, 71%, based on $H_2$obb). Elemental analysis calcd (%) for **3**: C 53.98, H 4.18, N 5.59; found C 53.84, H 4.41, N 5.98.

**X-ray Crystallographic Study.** The diffraction data for compounds were collected on an Oxford Xcalibur diffractometer equipped with a graphite−monochromatized Mo−K$\alpha$ radiation ($\lambda$ = 0.71073 Å) at 293(2) K. **Crystal data for 1-Zn**: $C_{34}H_{29}N_2O_{12}Zn_2$, $M$ = 788.33, monoclinic, $a$ = 27.3020(13) Å, $b$ = 15.9448(6) Å, $c$ = 21.0207(12) Å, $\beta$ = 95.461(4)°, $V$ = 9109.3(8) Å $^3$, $T$ = 293(2) K, space group $C2/c$, $Z$ = 8, 13939 reflections measured, 2494 independent reflections ($R_{int}$ = 0.0693). The final $R_1$ value was 0.1281 ($I > 2\sigma(I)$). The final $wR(F^2)$ value was 0.3489 ($I > 2\sigma(I)$). The goodness of fit on $F^2$ was 1.058. The high $R_1$ value is due to the large porous feature of the framework with structurally disordered guest molecules. **Crystal data for 2**: $C_{41}H_{24}N_3O_{11}Zn_2$, $M$ = 865.41, orthorhombic, $a$ = 16.7758(6) Å, $b$ = 11.0644(3) Å, $c$ = 22.4317(8) Å, $V$ = 4163.6(2) Å$^3$, $T$ = 293(2) K, space group $Pcca$, $Z$ = 4, 7219 reflections measured, 3044 independent reflections ($R_{int}$ = 0.0246). The final $R_1$ value was 0.0558 ($I > 2\sigma(I)$). The final $wR(F^2)$ value was 0.1597 ($I > 2\sigma(I)$). The goodness of fit on $F^2$ was 1.088. **Crystal data for 3**: $C_{36}H_{27}Cu_2N_2O_{11}$, $M$ = 790.68, monoclinic, $a$ = 33.025(7) Å, $b$ = 15.919(3) Å, $c$ = 20.831(5) Å, $\beta$ = 122.187(7)°, $V$ = 9268(3) Å$^3$, $T$ = 293(2) K, space group $C2/c$, $Z$ = 8, 17608 reflections measured, 6020 independent reflections ($R_{int}$ = 0.0643). The final $R_1$ value was 0.1162 ($I > 2\sigma(I)$). The final $wR(F^2)$ value was 0.3225 ($I > 2\sigma(I)$). The goodness of fit on $F^2$ was 1.109. The high $R_1$ value is due to the large porous feature of the framework with structurally disordered guest molecules. The structures were solved by the direct method and refined by the full-matrix least-squares on $F^2$ using the SHELXTL-97 program.

## RESULTS AND DISCUSSION

Compound **1-Zn** was solvothermally synthesized by heating a solution of $Zn(NO_3)_2\cdot 6H_2O$ and $H_2$obb in DMF/EtOH at 80 °C for five days. Single-crystal X-ray diffraction reveals that **1-Zn** crystallizes in the space group $C2/c$. There are two crystallographically independent $Zn^{2+}$ ions and two deprotonated obb$^{2-}$ ligands in each formula unit. Each V-shaped obb ligand connects two pairs of independent $Zn^{2+}$ ions through two carboxylate ends. Two symmetry-related $Zn^{2+}$ ions are bridged by four carboxylate groups of four obb ligands to form a common paddle wheel unit. Since each $Zn^{2+}$ ion has square-pyramidal coordination geometry, its axial position is further coordinated by a solvent DMF molecule (Figure 1a). Because

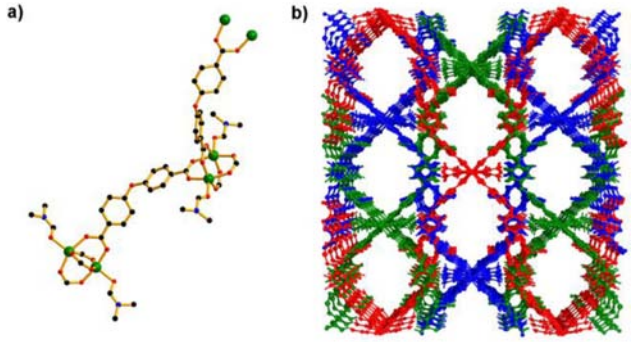


**Figure 1.** a) The coordination environment in **1-Zn** and b) view of the 3-fold interpenetrating framework in **1-Zn** along the $c$-axis.

of the V-shaped nature of the obb linkers, they bridge the resulting $Zn_2(COO)_4$ units into a complicated three-dimensional network with very open channels along the $c$-axis (Figure 1b). The rhombic window of a channel consists of eight $Zn_2(COO)_4$ units and eight obb ligands, which shows a large dimension about 47.8 × 27.3 Å$^2$. Such a framework can be topologically represented as a 4-connected **pts** net by reducing two kinds of $Zn_2(COO)_4$ units as two kinds of nodes and the obb ligands as the linkers (Figure S2).[7] Another Zn-obb compound MCF-22 has been reported previously, but MCF-22 possessed a distinct 4-connected **lvt** topological network.[8] 3-Fold framework interpenetration is also found for this open structure of **1**, but its whole structure still has channels with effective window size 7 × 8 Å$^2$ along the $c$-axis (Figure 1b). The large free spaces in **1-Zn** are occupied by coordinated DMF molecules and structural disordered solvent molecules. The void volumes of **1** with and without coordinating DMF molecules are 35.8% and 53.8%, respectively, as estimated by the PLATON program.

Thermogravimetric analysis (TGA) on the as-synthesized sample of **1-Zn** indicated a weight loss of 30.85% in the temperature range 20−230 °C, which is consistent with the release of two coordinating DMF molecules and two DMF guest molecules (calc. 31.23%) per formula unit (Figure S3). The TGA of the $CH_2Cl_2$-exchanged sample (**1a-Zn**) prepared by soaking **1-Zn** in $CH_2Cl_2$ shows that all of the structural disordered guests can be completely exchanged by $CH_2Cl_2$. The powder X-ray diffraction (PXRD) pattern of desolvated solid (**1-Zn-ht**), prepared by heating **1a-Zn** at 100 °C for 8 h under vacuum, indicates that framework distort or structural transformation may occur, because the peaks are obviously changed as compared to that of the as-synthesized sample of **1-Zn** (Figure 2). Notably, the origin open structure of **1-Zn** can be restored after **1-Zn-ht** is reimmersed in DMF for one day, as evidenced by PXRD patterns. However, further gas sorption measurements reveal that **1-Zn-ht** is hard to adsorb any gas, such as $N_2$, $H_2$, and $CO_2$ (Figure S4). The above results may conclude that compound **1-Zn** is a flexible framework and tends to shrink without the sustainers.

When $Cu(NO_3)_2$ was used to replace $Zn(NO_3)_2$ for the synthesis, **1-Cu** can be obtained, and it is isostructural to **1-Zn**. Compared to the as-synthesized sample of **1-Zn**, the XRD


dx.doi.org/10.1021/ic300778m | Inorg. Chem. 2012, 51, 9649−9654

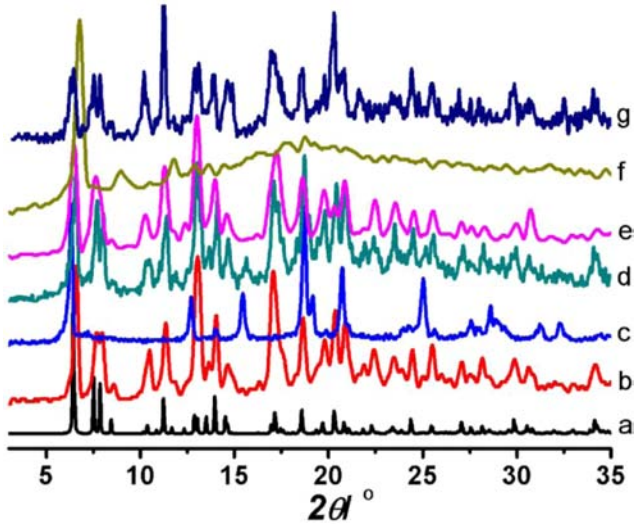


**Figure 2.** PXRD patterns: simulated from the single-crystal data of **1-Zn** (a), as-synthesized **1-Zn** (b), desolvated **1-Zn-ht** obtained by heating **1a-Zn** at 30 °C for 12 h under vacuum (c) and resolvated **1-Zn-DMF** prepared by immersing **1-Zn-ht** in DMF (d), as-synthesized **1-Cu** (e), desolvated **1-Cu-ht** obtained by heating **1a-Cu** at 100 °C for 12 h under vacuum (f) and resolvated **1-Cu-DMF** prepared by immersing **1-Cu-ht** in DMF (g).

pattern of **1-Cu** indicates it has the same porous framework with **1-Zn** (Figure 2e). The TGA of MeOH-exchanged sample (**1a-Cu**) prepared by soaking **1-Cu** in MeOH shows that all of the structural disordered guests and coordinated DMF molecules can be completely exchanged by MeOH (Figure S5). A desolvated solid (**1-Cu-ht**) was prepared by heating **1a-Cu** at 100 °C for 8 h under vacuum. For different guest-loading **1-Cu**, its PXRD patterns and gas sorption behaviors are similar to that of **1-Zn** (Figures 2f-g and S6). The results indicate that the simple replacement of metal centers does not help for the stability of such a flexible porous framework.

Thus, our further effort is trying to add the sustainers, such as the rigid 4,4′-bpy ligand, to support the pores. The solvothermal reaction of $Zn(NO_3)_2{\cdot}6H_2O$, $H_2$obb, and 4,4′-bpy under the similar conditions of **1** was performed, but a new compound **2** with distinct structural feature was obtained. The structure of **2** also consists of similar dinuclear paddle-wheel $Zn_2(COO)_4$ units which are linked by both obb ligands and 4,4′-bpy ligands (Figure 3a). However, the V-shaped bridging obb ligands in **2** only connect such $Zn_2(COO)_4$ units into a grid-like $4^4$ Zn-obb layer, and the resulting layers are further pillared by the 4,4′-bpy ligands via the axial coordination of each Zn atom, forming a pillared layer structure. 2-Fold interpenetration is presented in the whole framework (Figure 3b). Each single framework can be topologically represented as a uninodal 6-connect **rob** net by reducing each $Zn_2(COO)_4$ unit into a 6-connected node.[7] After interpenetration, the whole framework still shows open channels with small triangular apertures (the effective window size of 3.5 × 3.5 $Å^2$), and the void volume calculated by PLATON program is 26.3% of the total crystal volume.

Viewed from the TGA curve of **2**, the first weight loss of 8.18% in the range of 25−230 °C corresponds to the loss of one guest DMF molecule per formula unit (calc. 8.36%). No further weight loss is observed until 350 °C (Figure S9). The guest-free compound (**2-ht**) underwent a minor structure change after evacuation at 150 °C under dynamic vacuum for 5 h, as confirmed by PXRD analysis (Figure 4).

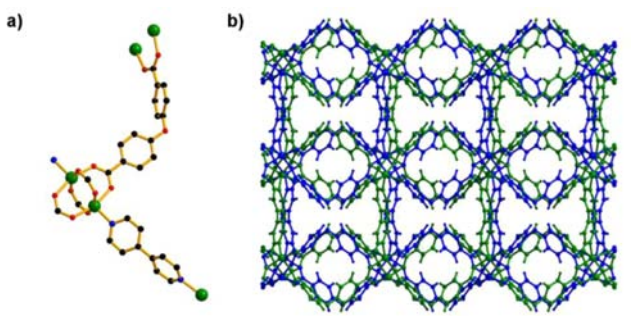


**Figure 3.** a) The coordination environment in **2** and b) view of the 2-fold interpenetrating framework of **2** along the *a*-axis.

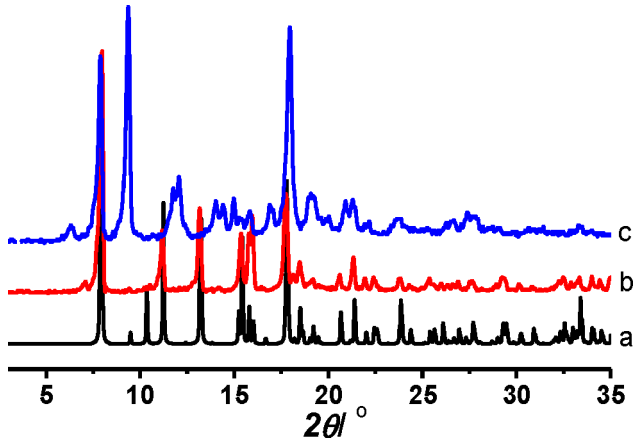


**Figure 4.** PXRD patterns: simulated from the single-crystal data of **2** (a), as-synthesized **2** (b), and desolvated **2-ht** (c) obtained by heating **2** at 150 °C for 12 h under vacuum.

Considering that Cu(II) centers may be more propitious to form paddle-wheel units, the replacement of Zn(II) in **1** with Cu(II) is possible to produce isostructural compound. Thus, a deliberate solvothermal assembly of $Cu(NO_3)_2{\cdot}6H_2O$, obb, and 4,4′-bpy generated our aimed product **3**. In the structure of **3**, there are two independent paddle-wheel $Cu_2(COO)_4$ units. One unit is covered by two coordinated DMF molecules and acts as a 4-connected node, while another unit is coordinated by two 4,4′-bpy ligands and acts as a 6-connected node (Figure 5a). The $\mu_4$-obb ligands link the $Cu_2(COO)_4$ units into a 3-fold

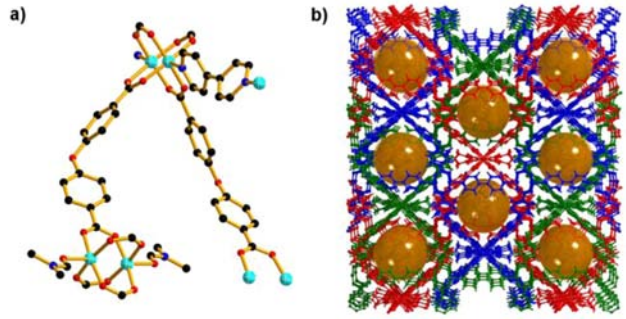


**Figure 5.** a) The coordination environment in **3** and b) view of the 3-fold interpenetrating framework of **3** along the *c*-axis. The free spaces in the framework are presented as orange balls.


dx.doi.org/10.1021/ic300778m | *Inorg. Chem.* 2012, 51, 9649−9654

interpenetrating open framework which exhibits very similar porous structure with compound **1** along the *c* axis (Figure 5b). One obvious difference between **1** and **3** is that some coordinated DMF molecules in big rhombic channels of **1** have been substituted by the bridging 4,4′-bpy ligands in **3** (Figure 6).

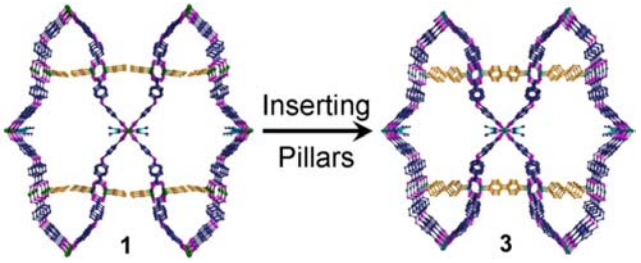


**Figure 6.** The structural difference between two simple frameworks of **1** and **3**.

Topological analysis indicates that one simple framework of **3** features an unusual binodal (4,6)-connected **seh** topology when the paddle-wheel units are simplified as 4-connected and 6-connected nodes, respectively (Figure S7).[7] Notably, if the 4,4′-bpy linkers are omitted, the simple Cu-obb framework has 4-connected **lvt** topology which is similar to MCF-22.[8] It is clear now that this (4,6)-connected **seh** net can be derived from a **lvt** net through inserting additional linkers. Although 3-fold interpenetration is formed to avoid an extremely large void space, **3** still possesses a significant solvent accessible space. Actually, disordered DMF guest molecules were found in the irregular rectangular channels. The effective window size of each channel in **3** is 4 × 8 Å$^2$, which is larger than that in **2**. Taking into account the guest solvent molecules as well as the coordinated DMF molecules, the solvent-accessible volume in **3** is estimated to be 45.6% of the unit cell volume, among them 35.8% occupied by disordered DMF guest molecules.

TGA of **3** reveals 24.17% weight loss from 25 to 260 °C (Figure S11), which corresponds to the loss of all DMF molecules in the framework (calc. 24.31%). The host framework starts to decompose rapidly from 285 °C. The high eliminating temperature of DMF might be related to the cage-like cavity of the structure. For gas adsorption studies, the sample of **3** was completely exchanged by methanol, and the methanol-exchanged sample was further activated by heating at 100 °C for 8 h under vacuum, giving a hollow framework **3-ht**. The PXRD pattern of **3-ht** is coincident with that of the simulated pattern derived from the X-ray single-crystal raw data, which confirms that integrity of the framework is maintained upon solvent removal (Figure 7). These results reveal that the framework structure of **3** becomes much rigid and stable under the help of additional 4,4′-bpy pillars.

To verify the porosity of solid **2-ht** and **3-ht**, gas sorption isotherms were measured with $N_2$, $H_2$, $CO_2$, and $CH_4$. Solid **3-ht** adsorbs $N_2$ to show a reversible type I isotherm, which indicates a permanent microporosity (Figure 8). However, **2-ht** does not sorption $N_2$ because of the size-exclusion effect ($N_2$ kinetic diameter: 3.6 Å). Solid **3-ht** shows $N_2$ uptake of approximately 228 cm$^3$·g$^{-1}$ (STP) at 1 bar. The BET and Langmuir surface areas of **3-ht** are estimated to be 829 m$^2$·g$^{-1}$ and 906 m$^2$·g$^{-1}$, respectively. Pore size distribution based on Horvath–Kawazoe (H–K) model gives a pore diameter of 9.0 Å. The measured pore volume (0.337 cm$^3$·g$^{-1}$) from the $N_2$ sorption was slightly higher than that (0.316 cm$^3$·g$^{-1}$) estimated from the single crystal structure, which indicated that the $N_2$ molecules in the pore were compressed to a greater extent than in the liquid nitrogen at 77 K.[9]

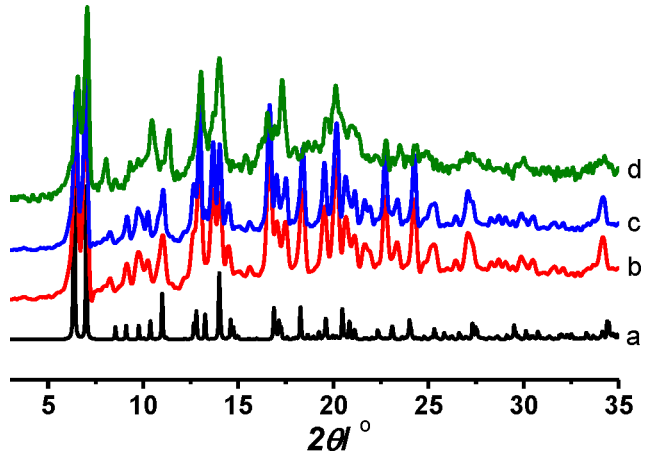


**Figure 7.** PXRD patterns: simulated from the single-crystal data of **3** (a), as-synthesized **3** (b), MeOH-exchanged **3a** (c), and desolvated **3-ht** (d) obtained by heating **3a** at 100 °C for 12 h under vacuum.

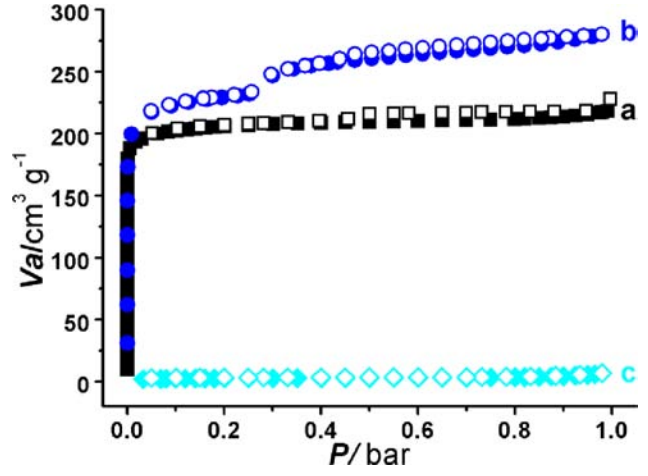


**Figure 8.** Gas sorption isotherms for **2-ht** and **3-ht**: (a) $N_2$ at 77 K for **3-ht**, (b) Ar at 87 K for **3-ht**, and (c) $N_2$ at 77 K for **2-ht**.

To further explore their potential properties on gas separation under ambient conditions, the adsorption isotherms of $CO_2$, $CH_4$, and $N_2$ for **2-ht** and **3-ht** were measured. Under 273 K and 1 bar, **3-ht** can hardly adsorb $N_2$ (2.9 cm$^3$·g$^{-1}$) (Figure 9f), but the capacity of $CO_2$ for **3-ht** are 65.9 cm$^3$·g$^{-1}$ at 273 K and 36 cm$^3$·g$^{-1}$ at 298 K and that of **2-ht** are 24 and 17 cm$^3$·g$^{-1}$, respectively (Figure 9a-c, 9e). The enthalpy of $CO_2$ adsorption for **2-ht** and **3-ht** were estimated from the sorption isotherms at 273 and 298 K using the virial equation to understand the strong affinity toward $CO_2$. At zero coverage, the enthalpy of $CO_2$ adsorption is 26.5 kJ/mol for **2-ht** and 21.3 kJ/mol for **3-ht**. The higher enthalpy of $CO_2$ adsorption for **2-ht** can be attributed to its narrow pores. The initial slopes of the $CO_2$ and $N_2$ adsorption isotherms were calculated, and the ratios of these slopes were used to estimate the adsorption selectivity for $CO_2$ over $N_2$ (Figure S19).[10] From these data, the calculated $CO_2/N_2$ selectivity is 30:1 at 273 K. In addition, the capacity of **3-ht** to adsorb $CH_4$ is 19.2 cm$^3$·g$^{-1}$ (1.4 wt %) and much less than that of $CO_2$ (65.9 cm$^3$·g$^{-1}$, 12.9 wt %)


dx.doi.org/10.1021/ic300778m | Inorg. Chem. 2012, 51, 9649–9654

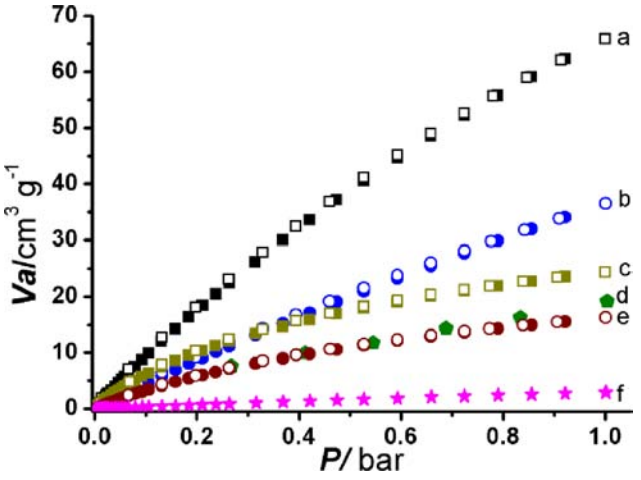


**Figure 9.** Gas sorption isotherms for **2-ht** and **3-ht**: (a) $CO_2$ at 273 K for **3-ht**, (b) $CO_2$ at 298 K for **3-ht**, (c) $CO_2$ at 273 K for **2-ht**, (d) $CH_4$ at 273 for **3-ht**, (e) $CO_2$ at 298 K for **2-ht**, and (f) $N_2$ at 273 for **3-ht**.

under the same conditions (Figure 9d), but at 72 bar, the uptake of $CH_4$ can reach 125.4 $cm^3 \cdot g^{-1}$ (9.0 wt %, Figure S20).

Both $H_2$ sorption isotherms at 77 and 87 K of **3-ht** show type I behavior (Figure 10). Note that the adsorption and

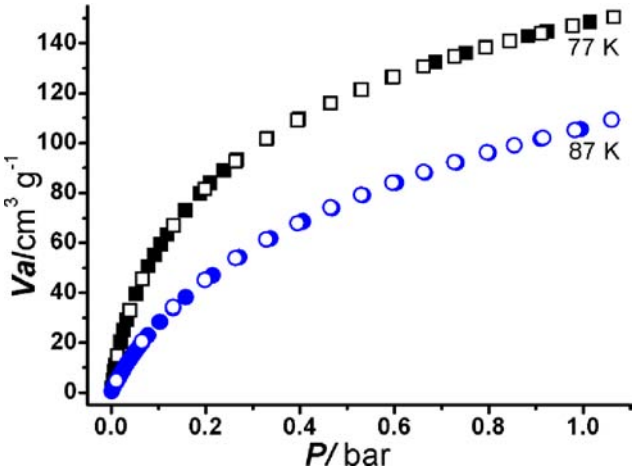


**Figure 10.** $H_2$ sorption isotherms for **3-ht** recorded at 77 and 87 K.

desorption isotherm curves overlap with each other with no hysteresis and no noticeable change in the properties upon repeated cycling. At 77 K and 1 bar, solid **3-ht** adsorbs $H_2$ up to 150.4 $cm^3 \cdot g^{-1}$ (1.34 wt %). Under the same conditions, the fraction of the pore volume filled by liquid $H_2$ ($\rho_{H2}$ = 0.0708 g/$cm^3$) at 1 atm and 77 K for **3-ht** is 55.7%, notably higher than the corresponding values for MOF-5 (13.7%), IRMOF-2 (19.2%), IRMOF-6 (18.3%), IRMOF-11 (31.4%), IRMOF-13 (33.5%), and IRMOF-20 (12.5%) but lower than that of IRMOF-74 (64.1%).[11] Moreover, the $H_2$ adsorption enthalpy ($Q_{st}$) calculated by the virial equation from the adsorption isotherms measured at 77 and 87 K is 7.0 $kJ \cdot mol^{-1}$. Because the $H_2$ sorption isotherm of **3-ht** is not fully saturated at 1 bar, a higher $H_2$ sorption capacity may be expected under higher pressures.

The sorption isotherms of benzene and cyclohexane vapor for **3-ht** also were measured at room temperature (Figure 11). The amount of benzene adsorbed by **3-ht** is 20.6 wt %, a value

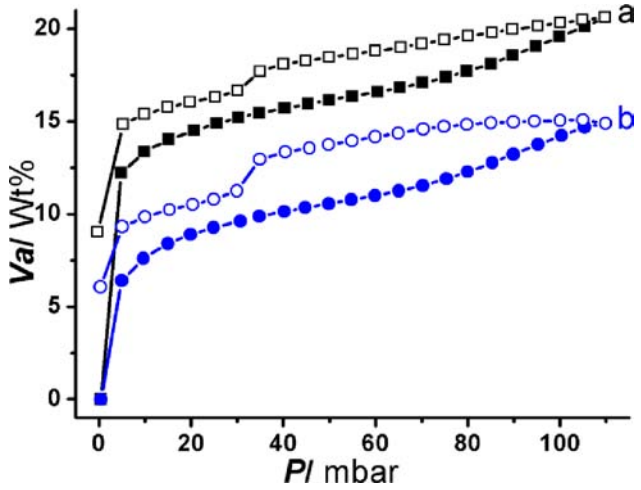


**Figure 11.** Benzene (a) and cyclohexane (b) sorption isotherms of **3-ht** recorded at 298 K.

surpassing that of cyclohexane (14.9 wt %). Remarkable, large hysteresis loops without complete desorption were observed in the both sorption isotherms of benzene and cyclohexane. It is possible to physically lock (imprison or encapsulate) guest molecules in a cage-like container with a diameter of approximate 0.9 nm, inducing strong sorbate–sorbent interactions to incomplete desorption.[12]

## CONCLUSION

By varying degrees of success on increasing the connectivity of the bridging bpy ligands, three new M(II)-4,4′-oxybisbenzoic frameworks with distinct framework topologies and comparable thermal stability are successfully synthesized. It is interesting the flexible framework of **1-Zn** and **1-Cu** can hardly adsorb any gas, but the rigid framework of **3** exhibits gas selective uptake of $CO_2$ over $N_2$ and $CH_4$. For **3**, it has $CO_2$ uptake of 65.9 $cm^3 \cdot g^{-1}$ under 273 K and 1 bar but only 2.9 $cm^3 \cdot g^{-1}$ for $N_2$ and 19.2 $cm^3 \cdot g^{-1}$ for $CH_4$. An interesting physically lock effect is also observed in benzene and cyclohexane sorption for **3**. The results reveal a successful example of tuning MOF stability and porosity via adding rigid pillars into flexible frameworks.

## ASSOCIATED CONTENT

### Supporting Information

Additional figures, TGA, gas sorption isotherms, isosteric heat isotherms, and CIF files. This material is available free of charge via the Internet at http://pubs.acs.org.

## AUTHOR INFORMATION

### Corresponding Author

*E-mail: zhj@fjirsm.ac.cn.

### Funding

This work was supported by the National Basic Research Program of China (973 Programs 2012CB821705 and 2011CB932504), NSFC (21073191), NSF of Fujian Province (2011J06005), and CAS and SRF for ROCS, SEM.

### Notes

The authors declare no competing financial interest.

## REFERENCES

(1) (a) Férey, G. *Chem. Soc. Rev.* **2008**, *37*, 191. (b) ÓAlessandro, D. M.; Smit, B.; Long, J. R. *Angew. Chem., Int. Ed.* **2010**, *49*, 6058.

(c) Zhao, D.; Yuan, D.; Zhou., H.-C. *Energy Environ. Sci.* **2008**, *1*, 222. (d) Li, J.-R.; Sculley, J.; Zhou, H.-C. *Chem. Rev.* **2012**, *112*, 869. (e) Zeng, M.-H.; Wang, Q.-X.; Tan, Y.-X.; Hu, S.; Zhao, H.-X.; Long, L.-S. *J. Am. Chem. Soc.* **2010**, *132*, 2561. (f) Yin, Z.; Wang, Q.-X.; Zeng, M.-H. *J. Am. Chem. Soc.* **2012**, *134*, 4857. (g) Yang, S.; Lin, X; Lewis, W.; Suyetin, M.; Bichoutskaia, E.; Parker, J. E.; Tang, C. C.; Allan, D. R.; Rizkallah, P. J.; Hubberstey, P.; Champness, N. R.; Thomas, K. M.; Blake, A. J.; Schröder, M. *Nat. Mater.* **2012**, *11*, 710.

(2) (a) Serra-Crespo, P.; Ramos-Fernandez, E. V.; Gascon, J.; Kapteijn, F. *Chem. Mater.* **2011**, *23*, 2565. (b) Gustafsson, M.; Bartoszewicz, A.; Martín-Matute, B.; Sun, J.; Grins, J.; Zhao, T.; Li, Z.; Zhu, G.; Zou, X. *Chem. Mater.* **2010**, *22*, 3316. (c) Fei, H.; U, L. P.; Rogow, D. L.; Bresler, M. R.; Abdollahian, Y. A.; Oliver, S. R. J. *Chem. Mater.* **2010**, *22*, 2027. (d) Wang, X.-S.; Meng, L.; Cheng, Q.; Kim, C.; Wojtas, L.; Chrzanowski, M.; Chen, Y.-S.; Zhang, X. P.; Ma, S. *J. Am. Chem. Soc.* **2011**, *133*, 16322. (e) Ma, S.; Meng, L. *Pure Appl. Chem.* **2011**, *83*, 167. (f) McDonald, T. M.; Lee, W. R.; Mason, J. A.; Wiers, B. M.; Hong, C. S.; Long, E. R. *J. Am. Chem. Soc.* **2012**, *134*, 7056.

(3) (a) Suh, M. P.; Cheon, Y. E.; Lee, E. Y. *Chem.—Eur. J.* **2007**, *13*, 4208. (b) Yazaydın, A. Ö.; Benin, A. I.; Faheem, S. A.; Jakubczak, P.; Low, J. J.; Willis, R. R.; Snurr, R. Q. *Chem. Mater.* **2009**, *21*, 1425. (c) Lin, Q.; Wu, T.; Zheng, S.; Bu, X.; Feng, P. *Chem. Commun.* **2011**, *47*, 11852. (d) Zheng, S.; Bu, J. J.; Wu, T.; Chou, C.; Feng, P.; Bu, X. *Angew. Chem., Int. Ed.* **2011**, *50*, 8858. (e) Chen, L.; Bu, X. *Chem. Mater.* **2006**, *18*, 1857.

(4) (a) Kitagawa, S.; Uemura, K. *Chem. Soc. Rev.* **2005**, *34*, 109. (b) Guo, Z.; Wu, H.; Gadipelli, S.; Liao, T.; Zhou, Y.; Xiang, S.; Chen, Z.; Yang, Y.; Zhou, W.; O'Keeffe, M.; Chen, B. *Angew. Chem., Int. Ed.* **2011**, *50*, 3178. (c) Chen, B.; Xiang, S.; Qian, G. *Acc. Chem. Res.* **2010**, *43*, 1115.

(5) (a) Rowsell, J. L. C.; Yaghi, O. M. *J. Am. Chem. Soc.* **2006**, *128*, 1304. (b) Sun, D.; Ma, S.; Ke, Y.; Petersen, T. M.; Zhou, H.-C. *Chem. Commun.* **2005**, 2663. (c) Ma, S.; Zhou, H.-C. *J. Am. Chem. Soc.* **2006**, *128*, 11734. (d) Ma, S.; Wang, X.; Yuan, D.; Zhou, H.-C. *Angew. Chem., Int. Ed.* **2008**, *47*, 4130.

(6) (a) Park, H. J.; Lim, D.-W.; Yang, W. S.; Oh, T.-R.; Suh, M. P. *Chem.—Eur. J.* **2011**, *17*, 7251. (b) Nelson, A. P.; Farha, O. K. K.; Mulfort, L.; Hupp, J. T. *J. Am. Chem. Soc.* **2009**, *131*, 458. (c) Ma, L.; Jin, A.; Xie, Z.; Lin, W. *Angew. Chem., Int. Ed.* **2009**, *48*, 9905.

(7) (a) Blatov, V. A.; Carlucci, L.; Ciani, G.; Proserpio, D. M. *CrystEngComm* **2004**, *6*, 377. (b) Alexandrov, E. V.; Blatov, V. A.; Kochetkov, A. V.; Proserpio, D. M. *CrystEngComm* **2011**, *12*, 3947.

(8) Xue, D.-X.; Lin, J.-B.; Zhang, J.-P.; Chen, X.-M. *CrystEngComm* **2009**, *11*, 183.

(9) Park, M.; Moon, D.; Yoon, J. W.; Chang, J.-S.; Lah, M. S. *Chem. Commun.* **2009**, 2026.

(10) An, J.; Geib, S. J.; Rosi, N. L. J. *Am. Chem. Soc.* **2010**, *132*, 38.

(11) (a) Wong-Foy, A. G.; Matzger, A. J.; Yaghi, O. M. *J. Am. Chem. Soc.* **2006**, *128*, 3494. (b) Panella, B.; Hirscher, M.; Püller, H. *Adv. Funct. Mater.* **2006**, *16*, 520. (c) Rowsell, J. L. C.; Yaghi, O. M. *J. Am. Chem. Soc.* **2006**, *128*, 1304.

(12) Lan, A.; Li, K.; Wu, H.; Kong, L.; Nijem, N.; Olson, D H.; Emge, T. J.; Chabal, Y. J.; Langreth, D. C.; Hong, M.; Li, J. *Inorg. Chem.* **2009**, *48* (15), 7165.